Final Draft
of the original manuscript:

Wang, L.; Lorenz, U.; Muench, M.; Stark, A.; Pyczak, F.:
Influence of alloy composition and thermal history on carbide precipitation in Gamma-based TiAl alloys
In: Intermetallics (2017) Elsevier

DOI: 10.1016/j.intermet.2017.05.006

Influence of alloy composition and thermal history on carbide precipitation in γ-based TiAl alloys

*Li Wang[1], Uwe Lorenz[1], Mathias Münch[2], Andreas Stark[1], Florian Pyczak[1,2]

[1]Institute of Materials Research, Helmholtz-Zentrum Geesthacht, Max-Planck-Strasse 1, Geesthacht, D-21502, Germany

[2]Brandenburgisch Technische Universität Cottbus-Senftenberg, Konrad-Wachsmann-Allee 17, Cottbus, D-03046, Germany

* Corresponding author: Tel.: +49 04152-87-2672; fax: +49 04152-87-2534

E-Mail: Li.wang1@hzg.de (Li Wang)

Abstract

Carbide precipitation in TiAl alloys with different alloying element additions and thermal history was investigated by transmission electron microscopy and high energy X-ray diffraction. The results reveal that Nb addition in TiAl alloys does not increase the carbon solubility in the γ matrix significantly. With increasing carbon concentration in the alloys, a splitting of the P-type carbides takes place earlier in the course of ageing at 800 °C and the formation of H-type carbides is promoted. For a nearly single γ phase alloy Ti-51Al-5Nb-0.5C, H-type carbides are the thermodynamically stable phase. However, with decreasing Al concentration, P-type carbides become thermodynamically stable at low carbon concentration (below 1%) in Ti-45Al and Ti-45Al-5Nb alloys. It is feasible to achieve high thermodynamical stability of the P-type carbides in TiAl alloys through controlling alloying elements.

Keywords

A. Intermetallics; B. alloy design; B. phase stability; F. diffraction/scattering (electron, neutron and X-ray); F. electron microscopy, transmission

1. Introduction

TiAl alloys are promising materials for high-temperature structural applications and have been applied successfully in commercial aircraft GEnx^{TM} engines as low-pressure turbine blades due to their low weight and excellent mechanical properties [1]. To extend the useful service temperature range, further improvements on creep resistance can be achieved by adding carbon. The strengthening mechanism might be attributed to either solid-solution hardening [2-4] or precipitation hardening [5-12]. To date two types of carbides are reported to be effective for improving the mechanical properties of TiAl alloys [6, 8, 9]. These are perovskite (P-Ti_3AlC) type carbides with a similar crystal structure to the γ-TiAl phase and hexagonal (H-Ti_2AlC) type carbides. A survey of literature about TiAl alloys shows that P-type carbides are thought to be meta-stable and form within the temperature range of 750 to 900 °C [13, 14]. Owing to a smaller lattice misfit along the c-axis of the γ phase, they exhibit needle-like shape and grow preferentially along the $[001]_\gamma$ direction [13-15]. However, H-type carbides are reported to be thermodynamically more stable. With increasing ageing times or ageing temperatures P-type carbides should disappear and H-type carbides should form instead [13, 14]. Owing to the coarse particle size H-type carbides are less effective compared with the P-type carbides for improving the mechanical performance of TiAl alloys [12]. Thus, it is essential to improve the thermal stability of P-type carbides or to obtain finely dispersed H-type carbides. The size, distribution and morphology of carbides play an essential role in determining the mechanical properties of TiAl alloys. For high-temperature applications in aerospace and automotive fields it is important to determine the long-term stability of carbides in TiAl alloys. However, studies on this issue are limited or carbides have already lost stability after a short annealing time [2, 9, 13, 16-19]. Our recent publications [15, 20] reveal that P-type carbides are thermodynamically stable and undergo a morphology evolution in Ti-45Al-5Nb-0.5C and -0.75C alloys after ageing at 800 °C for over 1000 hours. More details about the situation after around 5000 hours annealing can be found in this paper.

The published studies on carbides in TiAl alloys mainly focused on binary alloys with high Al content or ternary or quaternary systems with alloying elements below 3 at.% [5, 9, 14, 16, 21, 22]. However, novel TiAl alloys with higher temperature capability have been developed, known as third-generation TiAl alloys,

such as TNB and TNM alloys [12, 23]. These alloys are characterized by lower Al contents and higher levels of β-stabilizing alloying elements, such as Nb and Mo. Nb can slow down the diffusion processes and refine microstructures [12, 23]. In addition Nb is reported to increase the carbon solubility in γ-TiAl alloys [24]. Thus, the resulting carbide precipitation behavior in these alloys should vary. Other factors can also influence the formation, shape and size of carbide precipitates, such as the carbon concentration and thermal history.

In this study alloys with a composition of Ti-45Al-5Nb-xC were investigated and compared to the Nb-free alloy Ti-45Al-0.5C, and to alloys with a higher Al content, Ti-51Al-5Nb-xC and Ti-51Al-xC, in order to understand the effects of alloying elements on carbide precipitation. Additionally, the long-term stability of carbides in the Ti-45Al-5Nb-xC, Ti-45Al-0.5C and Ti-51Al-5Nb-0.5C alloys was evaluated. The carbide microstructures are characterized by transmission electron microscopy combined with high-energy X-ray diffraction.

2. Experimental

The Ti-45Al-5Nb-xC alloys (x=0.5, 0.75 and 1.0, all in atomic percent throughout the paper) and the Ti-45Al-0.5C alloy were produced by powder metallurgy (PM). Pre-alloyed powders produced by the plasma melting induction guiding gas atomization (PIGA) technique were consolidated by hot isostatic pressing (HIP) at 1250 °C and 200 MPa for 2 h. Details about the powder production can be found in Ref. [25]. The actual carbon contents were measured to be 0.52, 0.74 and 0.97, at.% for the HIPed Ti-45Al-5Nb-xC alloys and 0.5 at.% for the HIPed Ti-45Al-0.5C alloy using the LECO CS-444 melt extraction system. The Ti-51Al-5Nb-xC (x=0, 0.01, 0.05 and 0.5, at.%) and Ti-51Al-xC (x=0, 0.01 and 0.025, at.%) alloys were produced by arc-melting method and specimens were re-melted for eight times to obtain chemical homogeneity. The actual carbon concentrations are 0.02, 0.03, 0.04 and 0.42, at.% in Ti-51Al-5Nb-xC alloys and 0.01, 0.016 and 0.02, at.% in Ti-51Al-xC alloys. For both PM and casting techniques, the starting materials were pure elements except for carbon which was added as TiC. The contents of oxygen and nitrogen in TiAl specimens after HIPing and casting are shown in **Table 1**.

To investigate the carbide precipitation in these alloys, specimens with a size of about 10mm×10mm×10mm were cut from the HIPed and cast billets, and heat treated at different temperatures and times, which is illustrated in **Table 2** [15]. For the Ti-45Al-5Nb-1.0C and Ti-51Al-5Nb-xC alloys, no solution treatment was applied prior to the annealing treatments. Concerning the Ti-45Al-5Nb-1.0C alloy, the primary H-type carbides at grain boundaries are thermally very stable and were not dissolved until heating up to 1400 °C, which was demonstrated by combining scanning electron microscopy and in-situ high-energy X-ray diffraction method. For cast Ti-51Al-5Nb-xC alloys, owing to the coarse grain size, the carbon enrichment at grain boundaries should not influence the carbon level in the grain interior significantly. Thus, these specimens were directly annealed without homogenizing treatment. For all alloys, annealing treatments were conducted under air. Samples after solution treatment at 1250 °C were oil quenched, while samples after annealing treatments between 800 and 1000 °C were furnace cooled.

High-energy X-ray diffraction (HEXRD) conducted at the HEMS and HARWI-II beam lines run by the Helmholtz-Zentrum Geesthacht at the Deutsches Elektronen-Synchrotron (DESY) in Hamburg, was used to analyze the lattice parameters and phase constitution of the alloys. The reflections were either recorded with a mar345 image plate or a PerkinElmer XRD 1622 flat panel detector at the HEMS beamline and a mar555 flat panel detector at HARWI-II. The phase fraction was obtained by Rietveld analysis of the high-energy X-ray diffraction patterns. Due to the low fraction of carbides, they were ignored when doing Rietveld refinement and only the main phases were analyzed.

Scanning electron microscopy (SEM) investigations were conducted using a LEO Gemini 1530. Specimens were cut, ground and then electro polished with a solution of 26 ml perchloric acid (70%), 359 ml 2-butanol and 625 ml methanol at 30 V and 30 ºC.

The microstructures, and here especially details about carbides were investigated by transmission electron microscopy (TEM) with a Philips CM200 Electron Microscope operated at 200 kV. The area density of the P-type carbides (number per unit area) was analyzed and averaged from three TEM images recorded along the [001] direction of the γ matrix. TEM foils with a diameter of 2.3 mm were first drilled,

ground to a thickness below 120 μm, and then thinned by twin-jet polishing at 25-35 V and a temperature of -40 °C with the same solution as used for SEM specimen preparation.

3. Results

The primary phase contents of the TiAl specimens are listed in **Table 2**. The microstructures of the HIPed heat-treated Ti-45Al-5Nb-xC alloys have been characterized elsewhere [15, 26]. They have a similar microstructure and are composed by the γ, α_2 and carbide phases. The amount and type of carbides depend on the carbon concentration in the alloy. The microstructure of the HIPed Ti-45Al-0.5C alloy is also composed of the γ and α_2 phases but the fraction of the α_2 phase is higher than that in the HIPed Ti-45Al-5Nb-0.5C alloy. The microstructure of the cast Ti-51Al-5Nb-xC and Ti-51Al-xC alloys consists mainly of the γ phase, together with a trace amount of the α_2 phase and a few primary P-type carbides depending on the carbon content.

The microstructures and phase fractions of the Ti-45Al-5Nb-0.5C and Ti-45Al-5Nb-0.75C alloys after heat treatment have been published in Ref. [15]. Both alloys have a similar microstructure and are composed of the γ, α_2 and P-type carbide phases. **Fig. 1a** shows an example of the microstructure of Ti-45Al-5Nb-0.5C after annealing at 800 °C for 168 h. Compared to the samples which were directly annealed at temperatures between 800 to 1000 °C, specimens which were previously solution heat treated at 1250 °C have a coarser grain size and more lamellar colonies with finer lamellar spacing after annealing treatment, as shown in **Fig. 1b**. But the fraction of the α_2 phase was similar in the two heat-treatment conditions. The microstructure of the Ti-45Al-0.5C and Ti-45Al-5Nb-1.0C alloys is also similar to the Ti-45Al-5Nb-0.5C alloy for the same heat treatment conditions. But the α_2 phase fraction is higher in the Ti-45Al-0.5C alloy and lower in the Ti-45Al-5Nb-1.0C alloy compared with that in the Ti-45Al-5Nb-0.5C alloy. **Table 3** lists the fractions of the α_2 phase for specimens which have been investigated by HEXRD. For the Ti-51Al-5Nb-xC and Ti-51Al-xC alloys, after annealing at 800 °C their microstructure did not change obviously and is still composed of coarse γ grains, a few small α_2 grains and carbide particles depending on the carbon concentration and annealing time.

3.1 The influence of Nb

Fig. 2 shows the TEM micrographs of the evolution of the P-type carbides in the Ti-45Al-5Nb-0.5C and Ti-45Al-0.5C alloys after solution treatment at 1250 °C for 5 h and subsequently annealing at 800 °C. In these two alloys only P-type carbides exist, which is confirmed by both TEM and HEXRD. For all annealing times (up to 5000 h), P-type carbides retain the same orientation relationship (OR) with the γ matrix: $[100]_P$ // $[100]_\gamma$ and $(010)_P$ // $(010)_\gamma$ as reported in literature [13, 14]. TEM micrographs in **Fig. 2** were recorded from the [001] and [100] directions to better observe the morphology development. For both alloys at the beginning of annealing at 800 °C, needle-shaped P-type carbides are formed in the γ grains and grow preferentially along the c-axis of the γ matrix.

With further annealing for 168 h, carbides grow and remain needle-like in the γ matrix of the Nb-free Ti-45Al-0.5C alloy (with an area density of $(0.44\pm0.10) \times 10^{15}$ m^{-2}). Thus, they show dot-like cross-sections viewed along the [001] direction (**Fig. 2a**). To compare with the Ti-45Al-5Nb-0.5C alloy after ageing for 168 h, most carbides in the matrix have also a needle-like morphology with a similar area density of $(0.45\pm0.05) \times 10^{15}$ m^{-2}. But we also see some assembled precipitates, as for example particle A in **Fig. 2b**.

Longer ageing time up to 1000 h, leads to a drastically decreased carbide density of around 0.02×10^{15} m^{-2} in the Ti-45Al-0.5C alloy. Moreover, the carbide projections in the [001] direction vary as displayed in **Fig. 2c**. For example, precipitate B shows moiré fringe pattern, but precipitate C only exhibits moiré fringes at the edge of the particle, while precipitate D is assembled from several small particles (accounted as one particle when measuring area density). The morphology of particle D is caused by carbide splitting and its mechanism has been discussed in [20]. However, in the Ti-45Al-5Nb-0.5C alloy, a higher carbide density of around 0.06×10^{15} m^{-2} (taking a sub-particle compound as one particle) in the γ grains can be detected (**Fig. 2d)**. Carbides have changed their morphology and split into small sub-particles. The conglomerates of sub-particles seem to have formed from split plates which were orientated with their former plate planes parallel to the $(100)_\gamma$ or $(010)_\gamma$ crystallographic planes. Based on the HEXRD patterns the fraction of the P-type carbides is determined to be about equal in both alloys after annealing for 1000 hours. It is noteworthy that these results do not indicate a significantly increased carbon solubility due to the Nb addition, which

is in contradiction to a previous study [24]. The influence of Nb on the carbon solubility in the γ matrix will be again discussed in the following when comparing the carbide formation in the Ti-51Al-5Nb-xC and Ti-51Al-xC alloys.

With further annealing for around 5000 h (**Fig. 2e** and **f**), in both alloys P-type carbides are still observable in the γ matrix. The former splitting structure is seldom observed anymore. Instead the morphology of the P-type carbides becomes irregular although some of them still tend to be elongated along the c-axis of the γ phase. Surrounding the precipitates a strong contrast can be seen, which may origin from the strain field. It should be noted that the precipitates now are often observed to be associated with dislocations.

3.2 The influence of C and Al

3.2.1 Two-phase Ti-45Al-5Nb-xC alloys

Based on the findings from our previous study [15], H-type carbides were not detected in the Ti-45Al-5Nb-0.5C and Ti-45Al-5Nb-0.75C alloys after annealing in the temperature range between 800 and 1000 °C. In the Ti-45Al-5Nb-0.5C alloys, P-type carbides form at 800 and 900 °C but dissolve at 1000 °C, while they exist in the Ti-45Al-5Nb-0.75C alloy after annealing at 800 to 1000°C. In comparison both P-type and H-type carbides have already formed in the HIPed Ti-45Al-5Nb-1.0C alloy. In the following, details about the development of carbides in the Ti-45Al-5Nb-1.0C alloy after annealing from 800 to 1000 °C are illustrated.

After ageing at 800°C for 24 h, P-type carbides in the Ti-45Al-5Nb-1.0C alloy are found to be needle-shaped and lie parallel to the $[001]_\gamma$ direction in the γ grains. They exhibit dot-like cross-sections when viewed along the [001] direction (**Fig. 3a**). With increasing annealing time to 48 h, the morphology of the P-type carbides gradually changes to plate-like (**Fig. 3b**). After annealing for 96 h it has been observed that the P-type precipitates start to split into finer sub-particles, as shown in **Fig. 3c**. This splitting phenomenon took also place in the Ti-45Al-5Nb-0.5 and Ti-45Al-5Nb-0.75C alloys but after longer annealing time of 168 h [15, 27]. Note that in the state after 1054 hours annealing parts of the carbides remain plate-shaped,

as shown for example in **Fig. 3d**. After annealing for around 5000 h (**Fig. 3e**), P-type carbides have an irregular morphology similar to the situation in the Ti-45Al-0.5C, Ti-45Al-5Nb-0.5C and Ti-45Al-5Nb-0.75C alloys described in section 3.1. The precipitates show moiré fringe contrast and dislocations are often observed surrounding them. These can be hints for a coherency loss between the P-type carbides and the γ phase. From the diffraction pattern in **Fig. 3e** it is evident that the OR still exists between the P-type carbides and the γ phase. After annealing the Ti-45Al-5Nb-1.0C alloy at 900 and 1000 °C, P-type carbides are present at grain boundaries, at dislocations and occasionally in the γ matrix after ageing at 900 °C for 168 h, while they are only found at grain boundaries and at dislocations after annealing at 1000 °C.

H-type carbides can also be detected at grain boundaries in the course of ageing between 800 to 1000 °C. But they have no orientation relationship with the surrounding γ grains. **Fig. 3f** shows an example of the H-type carbides at grain boundaries after annealing at 800 °C for 24 h, together with the diffraction pattern (**Fig. 3f**).

From the above results, it is concluded that P-type carbides are thermodynamically stable at low carbon concentrations (x≤0.75%). H-type carbides only form in the Ti-45Al-5Nb alloy with high carbon additions (x≥1%) and coexist with the P-type carbides at least in the temperature range of 800 to 1000 °C.

3.2.1 Nearly single-phase Ti-51Al-5Nb-xC and Ti-51Al-xC alloys

In another alloy series, Ti-51Al-5Nb-xC, with a higher aluminum concentration, after annealing at 800 °C for 168 h, P-type carbides were not observed in the variant with 0.02% carbon content (actual carbon content is used in this paragraph) but have precipitated at grain boundaries and at dislocations if the carbon content is increased to 0.03%. H-type carbides start to form at grain boundaries of the alloy variant with 0.04% carbon. In this alloy, in parallel with H-type carbides P-type carbides again exist at grain boundaries and at dislocations. Increasing carbon content to 0.42% leads to the formation of the H-type carbides not only at grain boundaries but also in the γ grains with plate-like shape. P-type carbides now are present at grain boundaries, at dislocations and in the γ matrix. Based on these results we can conclude that in Ti-

51Al-5Nb-xC alloys P-type carbides form at a lower carbon content (x≤0.04%) while H-type carbides are preferred to form at a higher carbon concentration (x≥0.04%).

The evolution of the carbides in the γ grains of the Ti-51Al-5Nb-0.5C alloy after annealing at 800 °C is shown in **Fig. 4**. After ageing for 24 h, P-type carbide are also observed to have needle-like shape elongated along the [001] direction. They show dot-like cross-sections when imaged along the [001] direction (**Fig. 4a**) and have an area density of about 1.6×10^{15} m^{-2}. The orientation relationship (OR) between P-type carbides and the γ phase: $[100]_P$ // $[100]_\gamma$ and $(010)_P$ // $(010)_\gamma$ is the same as found above for the Ti-45Al-5Nb-xC and Ti-45Al-0.5C alloys. With increasing ageing time to 48 h, a higher P-type carbide density of around 2.9×10^{15} m^{-2} is observed. Furthermore, they start to split into small particles (**Fig. 4b**). After annealing for 168 h, P-type carbides decompose and now smaller carbide sub-particles are visible (**Fig. 4c**).

H-type carbides have also formed in the γ grains after annealing at 800 °C for 24 h. They have a plate-like shape and their plate planes lie parallel to {111} planes of the γ grains. The orientation relationship between H-type carbides and the γ matrix is $[101]_\gamma$ // $[11\text{-}20]_H$, $\{111\}_\gamma$ // $(0001)_H$. **Fig. 4d** shows an example of the H-type carbides in the condition after annealing for 96 h. When imaged from the $[101]_\gamma$ direction, H-type carbides have four sets of projections H_1, H_2, H_3 and H_4. Projections H_1 and H_2 are from H-type carbide plates with plate planes parallel to $(11\text{-}1)_\gamma$ and $(1\text{-}1\text{-}1)_\gamma$ planes, respectively. Projections H_3 and H_4 stem from the ones which are inclined to the beam direction with plate planes parallel to $(111)_\gamma$ and $(\text{-}11\text{-}1)_\gamma$ planes. The arrangements of atoms in the $[0001]_H$ plane and the $\{111\}_\gamma$ plane are similar. Thus, the H phase nucleates with $(0001)_H$ plane parallel to the $\{111\}_\gamma$ plane to form a low-energy coherent or semi-coherent interface. When further annealing for around 5000 h, it is interesting to note that the numerous P-type carbides present at the early stage of ageing disappear completely in the γ grains. Instead only H-type carbides with a coarse size remain. The H-type carbide plates are still parallel to the {111} crystal plane of the γ phase and reveal four sets of projections when imaged along the $[110]_\gamma$ direction (**Fig. 4e**). From the diffraction pattern in **Fig. 4e** it is confirmed that H-type carbides retain the OR with the γ grains.

In the Ti-51Al-5Nb-0.5C alloy, H-type carbides are also present at grain boundaries. They develop in the course of ageing at 800 °C. After annealing for 24 h (**Fig. 5a**), H-type carbides at γ/γ grain boundaries

exhibit the same OR with one of the surrounding γ grains $[101]_{\gamma}$ // $[11\text{-}20]_{H}$, $\{111\}_{\gamma}$ // $(0001)_{H}$ as that of the H-type carbides in the γ grains. In addition, H phase is also detected around the few α_2 particles which are located at γ/γ grain boundaries. But these H-type carbides have no OR with the α_2 phase. With extended annealing for 168 h (**Fig. 5b**), no OR is found anymore between the H-type carbides and the surrounding γ grains. However, it is interesting to note that in **Fig. 5c** an OR between the H phase and the α_2 particle of $[10\text{-}10]_{H}$ // $[10\text{-}10]_{\alpha 2}$ and $(0001)_{H}$ // $(0001)_{\alpha 2}$ is observed. After comparing the case in **Fig. 5a** it is reasonable to assume that the H phase in conjunction with the α_2 particle in **Fig. 5c** is newly formed and may grow at the expense of the α_2 phase. The H-Ti_2AlC carbide phase has a hexagonal crystal structure as the α_2 phase. Meanwhile the chemical compositions of both phases have a similar Ti/Al elements ratio. During annealing, it is assumed the α_2 phase will gradually transform into H-type carbide phase which is the thermodynamically stable phase.

In the Ti-51Al-xC alloys after annealing for 168 hours at 800 °C, no carbides were observed with a carbon content of 0.01% (actual carbon content is used in this paragraph). When increasing the carbon concentrations to 0.016% and 0.02%, P-type carbides were found to form at dislocations in the γ matrix (**Fig. 6a**). Only one H-type carbide was observed in the Ti-51Al-0.016C alloy by TEM (**Fig. 6b**). It should be noted that the occurrence of the H-phase was not a typical feature but rather an exception in this alloy.

4. Discussions

4.1 Influence of alloying elements on carbide precipitation

4.1.1 Influence of Nb

The findings in the Ti-45Al-0.5C and Ti-45Al-5Nb-0.5C alloys imply that in Nb containing alloys the processes of carbide growth and coarsening have been changed compared to the Nb-free alloy. It is known that Nb slows down diffusion processes [12, 23], which may result in a sluggish kinetics of carbide precipitation and coarsening. This could be a reason why carbides are more stable in the γ grains of the Ti-45Al-5Nb-0.5C alloy. But the effect of the α_2 phase fraction cannot be ignored. From HEXRD it is found

that after 1000 hours annealing at 800 °C, the fractions of the α_2 phase are around 14.6 and 20.8 wt.% in Ti-45Al-5Nb-0.5C and Ti-45Al-0.5C alloys, respectively. As known from literature [28] the α_2 phase in TiAl alloys can dissolve more carbon than the γ phase. A higher α_2 phase fraction in the Nb-free alloy could accommodate a larger fraction of the overall carbon content and lead to a lower carbon concentration in the γ phase. Thus, carbides become unstable and dissolve in the γ phase. In conclusion Nb addition in TiAl alloys appears to have no obvious influence on the final carbide morphology. But it may stabilize the carbides in the γ grains by slowing down diffusion controlled morphology changes. How the effect of Nb to shift the phase fraction in favor of the γ phase may influence the stability of carbides is difficult to decide.

The nearly single γ phase Ti-51Al-5Nb-xC and Ti-51Al-xC alloys yield the opportunity to determine the carbon content of the γ phase itself with good precision which is experimentally highly demanding in the two-phase microstructures. Thus, direct conclusions about the effect of Nb on the carbon solubility in the γ phase can be drawn from the investigations in these single γ phase alloys. By comparing the carbide formation in the nearly single γ phase Ti-51Al-5Nb-xC and Ti-51Al-xC alloys, it can be concluded that Nb has not increased the carbon solubility in the γ phase significantly as carbides form in the Ti-51Al-5Nb alloy at carbon content above 0.02% and in the Ti-51Al alloy at around 0.016%. This point will be mentioned again in the following when the influence of Al is discussed.

4.1.2 Influence of C

In the two series of TiAl alloys under investigation, Ti-45Al-5Nb-xC and Ti-51Al-5Nb-xC, it is found that P-type and H-type carbides form at different carbon concentrations and different times. This fact might be due to different nucleation energies for the precipitates. The crystal structures of the P-type carbides and the γ matrix are similar. So at a given carbon concentration, P-type carbides would likely nucleate first. For higher carbon contents H-type carbides are found together with P-type carbides at the beginning of annealing. At least in one case, for the Ti-51Al-5Nb-0.5C alloy they are the only carbide type present after long-term annealing.

It was also found that depending on the carbon content, the splitting of carbides in the γ grains took place after different annealing times (168 h in Ti-45Al-5Nb-0.5C and Ti-45Al-5Nb-0.75C, 96 h in Ti-45Al-5Nb-1.0C, and 48 h in Ti-51Al-5Nb-0.5C). Generally speaking, increasing carbon concentration leads to an earlier splitting.

Qualitatively higher carbon contents promote the thermodynamic stability of H-type carbides and the onset of splitting of P-type carbides. Nevertheless, the exact carbon levels where H-type carbides become thermodynamically stable or the annealing time when splitting begins is also influenced by the overall alloy composition which was discussed for Nb in the section above and will be for Al in the section below.

4.1.3 Influence of Al

Comparing with the Ti-45Al-5Nb alloy, carbides form in the Ti-51Al-5Nb alloy at a very low carbon concentration (0.02%<x<0.03%). This is explained by the difference in phase composition. At a high Al content more γ and less α_2 phase is present. Thus, nearly all carbon present in the alloy is in the γ phase and carbide formation takes place at a relatively low overall carbon content due to the low carbon solubility in the γ phase. The microstructure of the Ti-45Al-5Nb-xC alloys is composed of the γ phase (≈84-90 wt.%) and the α_2 phase (≈10-16 wt.%). But Ti-51Al-5Nb-xC is nearly a single-phase alloy and consists mainly of the γ phase (≈98-99 wt.%). Based on the result that carbides are found at a carbon concentration of 0.02%<x<0.03% in the Ti-51Al-5Nb alloy, we estimate that the carbon solubility in the γ phase is in the range of 200 to 300 at.ppm. The carbon solubility in the Nb free Ti-51Al-xC alloys is also in this range as carbides were found at a carbon content of around 160 at.ppm, which agrees well with the value reported in the literature for a similar alloy without Nb [28]. Based on this experimental result and by comparison with literature it could be concluded that the addition of Nb did not increase the carbon solubility in the γ phase significantly. However there are some investigations by atom probe in TNB [24] and TNM [29] alloys implying that the carbon solubility in the γ phase is much higher than this value. The higher carbon solubility is attributed to the presence of Nb. The difference may be due to the fact that in these studies the

alloys were heat treated for several hours at much higher temperature (1050°C, eutectoid temperature) after hot-deformation.

Also splitting of P-type carbides begins already at 48 hours of annealing in Ti-51Al-5Nb-0.5C compared to 168 h in Ti-45Al-5Nb-0.5C. This may also be an effect of the total amount of carbon in Ti-51Al-5Nb-0.5C being present in the γ phase. There are other factors which may also affect the splitting process. In the Ti-51Al-5Nb-0.5C alloy, the density of carbides in the γ phase is relatively high. Thus, the stress fields overlap in the early stage of the precipitation process and if the splitting is an effect of internal stresses this may have an influence. In addition, a high Al addition decreases a_γ thus increases the lattice mismatch along a/b-axis, and increases c_γ thus decreases the lattice mismatch along c-axis. It was for example determined by HEXRD that the lattice parameters of the γ phase of Ti-45Al-5Nb-0.5C (heat treated 5 hours at 1250 °C and subsequently 1104 hours at 800 °C) are a = 0.40107 nm and c = 0.40722 nm. For Ti-51Al-5Nb-0.5C (heat treated 24 hours at 800 °C) a = 0.39992 nm and c = 0.40732 nm were found. Both factors can influence the strain condition of a single carbide particle. Moreover, in this alloy, the formation and growth of the H-type carbides competes with the precipitation of P-type carbides. All these factors can contribute to the difference in carbide splitting.

4.2 Comparison with literature studies

Table 4 summarizes the occurrence of carbides in the TiAl alloys investigated in this study at different annealing conditions. It is interesting to compare the results in this study with literature. In a Ti-49.75Al-0.5C alloy investigated by Tian et al. [8], P-type carbides were formed after annealing at 800 °C. By ageing at higher temperatures or for longer periods at 800 °C H-type carbides appeared and replaced the P-type carbides. In this study in Ti-51Al-5Nb-0.5C alloy (nearly single γ phase), both P- and H-type carbides are found after annealing at 800 °C for 24 h. With further annealing H-type carbides are stable over the time, while P-type carbides are dissolved. For TiAl alloys with high Al concentration (nearly single or single γ phase) at a carbon content of 0.5% P-type carbides are only meta-stable, while H-type carbides are the thermodynamically stable phase. In a two-phase Ti-48Al-2Nb alloy with a carbon content of about 600-

700 ppm investigated by Chen et al. [13], H-type carbides were also reported to be the thermodynamically stable phase and were formed at the expense of P-type carbides. Even after annealing at 750 or 815 °C for only 168 h, P-type carbides started to dissolve and H-type carbides formed instead at dislocations [13]. This agrees with the Ti-Al-C ternary phase diagrams available in literature [30-34]. They predict H-type carbides to be the thermodynamic equilibrium phase in alloys with Al concentration of 40 to 50 at.% between 750 and 1000 °C. However, in our study in the Ti-45Al-0.5C, Ti-45Al-5Nb-0.5C and Ti-45Al-5Nb-0.75C alloys with lower Al content, P-type carbides are found to be stable even after extended annealing times hinting that P-type carbides may be the thermodynamically stable phase in the temperature range between 800 and 900 °C. Only when the carbon content increases to 1.0%, H-type carbides form and coexist with the P-type carbides. This may be explained by the presence of the α_2 phase. The α_2 phase fraction slightly decreases with annealing (**Table 3**). The formation of the H-type carbides could be delayed or even no H-type carbides could be formed until enough carbon is released from the dissolving α_2 phase. The competitive relationship between the α_2 phase and the H-phase with respect to H-phase precipitation is also evidenced in the Ti-51Al-5Nb-0.5C alloy. With increasing annealing time at 800 °C, H-phase is found to form at the expense of the α_2 phase, as shown in **Fig. 5c**. The results of the Ti-51Al-0.01C and Ti-51Al-0.025C alloys contradict the phase diagram data available in literature. While the phase diagrams predict either no or H-type carbides to be stable depending on the carbon content for such high Al concentrations only P-type carbides or P- and H-type carbides were found in this alloy indicating that most probably a γ+P+H three phase region exists in this composition range. In this context, it is noteworthy that the thermodynamic description of the ternary Ti-Al-C system which is published in [32] is derived from experiments about the formation and stability of MAX-phases, i.e. considering specimens with significantly higher carbon content compared to the present study. This may already explain discrepancies between the experimental results presented here and the thermodynamic description of the Ti-Al-C system in [32] which could be not fully accurate for the low carbon contents investigated here. Thus, the results of this study may be useful for a further optimization of thermodynamic databases.

It is probable that with further increasing carbon concentration, P-type carbides become unstable or even only H-type carbides form even if the carbon concentration when this happens seems to be higher than reported until now. This is indicated by a study of Ayer et al. [35] in a Ti-44.5Al-6.64C alloy where they found the existence of the H-type carbides. From a technical point of view, it is interesting to note that higher amounts of carbon can be added to TiAl alloys with low Al content without losing the stability of P-type carbides which are desirable to improve the mechanical properties.

In all alloys investigated in this study the morphology evolution of the P-type carbides in the γ grains is more or less the same. As carbides grow they adjust their morphology to keep a low energy state. The morphology developed from needles to plates to configurations of split sub-particles. Finally, the elastic energy due to the lattice misfit between the P-type carbides and the γ phase increases significantly and thus the interface becomes semi-coherent or incoherent to release the energy. The step of carbide splitting was until now not found in other studies. Instead of carbide morphology change and carbide splitting as were observed in this work, Tian et al. [8] reported a long-range ordering of carbon-vacancies in the P-Ti_3AlC carbides and two ordered domains coexisting in a single needle after annealing at 800 °C. How the morphology variants of split up carbide compounds influence the mechanical properties of the material is an interesting point for investigation in further studies.

5. Conclusions

In this study, we investigated the carbide precipitation and carbide stability in TiAl alloys with varying alloying elements and thermal history. Different from what has been published in literature, P-type carbides can be the thermodynamically stable phase in the two-phase Ti-45Al and Ti-45Al-5Nb alloys when exposed to 800 °C for 5000 h. From a technical point of view, this finding is very important. Since H-type carbides in the two-phase TiAl alloys are likely to form only at grain boundaries at high carbon content, they seem to be useless for the improvement of the mechanical property. Thus, the high stability of the P-type carbides is essential for precipitation hardening. After annealing for 5000 h, carbides tend to lose coherency with the γ matrix. Whether they are still beneficial for strengthing will be examined in future work. To conclude,

based on these findings it is feasible to achieve high thermodynamic stability of the P-type carbides in TiAl alloys by controlling alloying elements.

- Nb addition in TiAl alloys does not increase the carbon solubility in the γ phase significantly but it may slow down the process of carbide precipitation and coarsening.
- Higher carbon concentration can lead to an earlier splitting of the P-type carbides and promote the formation of the H-type carbides. The actual overall carbon content where H-type carbides are stable depends on the alloy composition (0.5% for the nearly single-phase Ti-51Al-5Nb alloy and 1% for the two-phase Ti-45Al-5Nb alloy).
- In the course of ageing at 800 °C, P-type carbides retain the orientation relationship with the γ matrix no matter if located at grain boundaries or in the grain interior. They adjust their morphology from needles to plates and then split into smaller sub-particles. Finally, the shape becomes irregular and the carbides tend to lose coherency with the γ matrix.
- H-type carbides in the γ grains have a coarse particle size and exhibit a plate-like shape with the plate plane parallel to the {111} plane of the γ phase.

Acknowledgements

The authors are grateful to Dr. Michael Oehring and Dr. Jonathan Paul for fruitful discussions, and Dr. Frank-Peter Schimansky and Dirk Matthiessen for producing the specimen material investigated here. Li Wang acknowledges the funding from the Chinese Scholarship Council-Helmholtz program and the Helmholtz Postdoc program.

References

[1] B.P. Bewlay, M. Weimer, T. Kelly, A. Suzuki, P.R. Subramanian, The Science, Technology, and Implementation of TiAl Alloys in Commercial Aircraft Engines, MRS Online Proceedings Library, 1516 (2013) 49-58.

[2] B.D. Worth, Jones, J. W., Allison, J. E., Creep deformation in near-γ TiAl: II. influence of carbon on creep deformation in Ti-48Al-1V-0.3C, Metall Mater Trans A, 26 (1995) 2961-2972.

[3] R. Gerling, F.P. Schimansky, A. Stark, A. Bartels, H. Kestler, L. Cha, C. Scheu, H. Clemens, Microstructure and mechanical properties of Ti 45Al 5Nb + (0-0.5C) sheets, Intermetallics, 16 (2008) 689-697.

[4] F. Perdrix, M.F. Trichet, J.L. Bonnentien, M. Cornet, J. Bigot, Relationships between interstitial content, microstructure and mechanical properties in fully lamellar Ti-48Al alloys, with special reference to carbon, Intermetallics, 9 (2001) 807-815.

[5] P.I. Gouma, Davey, S. J., Loretto, M. H., Microstructure and mechanical properties of a TiAl-based powder alloy containing carbon, Mater Sci Eng, A, 241 (1998) 151-158.

[6] P.I. Gouma, Subramanian, K., Kim, Y. W., Mills, M. J., Annealing studies of γ-titanium aluminides alloyed with light elements for creep strengthening, Intermetallics, 6 (1998) 689-693.

[7] M. Karadge, Gouma, P. I., Kim, Y. W., Precipitation strengthening in K5-series γ-TiAl alloyed with silicon and carbon, Metall Mater Trans A, 34 (2003) 2129-2138.

[8] W.H. Tian, M. Nemoto, Effect of carbon addition on the microstructures and mechanical properties of γ-TiAl alloys, Intermetallics, 5 (1997) 237-244.

[9] U. Christoph, Appel, F., Wagner, R., Dislocation dynamics in carbon-doped titanium aluminide alloys, Mater Sci Eng, A, 239–240 (1997) 39-45.

[10] H.S. Park, S.K. Hwang, C.M. Lee, Y.C. Yoo, S.W. Nam, N.J. Kim, Microstructural refinement and mechanical properties improvement of elemental powder metallurgy processed Ti-46.6Al-1.4Mn-2Mo alloy by carbon addition, Metall Mater Trans A, 32 (2001) 251-259.

[11] E. Schwaighofer, B. Rashkova, H. Clemens, A. Stark, S. Mayer, Effect of carbon addition on solidification behavior, phase evolution and creep properties of an intermetallic β-stabilized γ-TiAl based alloy, Intermetallics, 46 (2014) 173-184.

[12] F. Appel, M. Oehring, R. Wagner, Novel design concepts for gamma-base titanium aluminide alloys, Intermetallics, 8 (2000) 1283-1312.

[13] S. Chen, P.A. Beaven, R. Wagner, Carbide precipitation in γ-TiAl alloys, Scr Metall Mater, 26 (1992) 1205-1210.

[14] W.H. Tian, T. Sano, M. Nemoto, Structure of perovskite carbide and nitride precipitates in $L1_0$-ordered TiAl, Philos Mag A, 68 (1993) 965-976.

[15] L. Wang, H. Gabrisch, U. Lorenz, F.P. Schimansky, A. Schreyer, A. Stark, F. Pyczak, Nucleation and thermal stability of carbide precipitates in high Nb containing TiAl alloys, Intermetallics, 66 (2015) 111-119.

[16] Y. Wu, Y.W. Park, H.S. Park, S.K. Hwang, Microstructural development of indirect-extruded TiAl-Mn-Mo-C intermetallic alloys during aging, Mater Sci Eng, A, 347 (2003) 171-179.

[17] P.I. Gouma, Mills, M. J. , Characterization of the precipitation process in a TiAl-based alloy with carbon and silicon additions, Philos Mag Lett, 78 (1998) 59-66.

[18] R.J. Simpkins II, M.P. Rourke, T.R. Bieler, P.A. McQuay, The effects of HIP pore closure and age hardening on primary creep and tensile property variations in a TiAl XD™ alloy with 0.1wt.% carbon, Mater Sci Eng, A, 463 (2007) 208-215.

[19] S.Q. Xiao, Foitzik, A. H., Pirouz, P., Heuer, A. H., Heterogeneous nucleation of Ti_2AIC precipitates at TiAl grain boundaries, Phys Status Solidi A, 131 (1992) 333-344.

[20] L. Wang, C. Zenk, A. Stark, P. Felfer, H. Gabrisch, U. Lorenz, F. Pyczak, Morphology evolution of Ti_3AlC carbide precipitates in high Nb containing TiAl alloys, in, 2017, submitted.

[21] P. Staron, U. Christoph, F. Appel, H. Clemens, SANS investigation of precipitation hardening of two-phase γ-TiAl alloys, Appl Phys A, 74 (2002) s1163-s1165.

[22] D. Seo, Y., Everard, T., McQuay, P. A., Bieler, T. R., The Effect of Carbon Concentration on Primary Creep of an Investment Cast Ti-47Al-2Mn-2Nb+0.8vol%TiB_2 Alloy, in: I. Baker, Noebe, R. D., George, E. P. (Ed.) Interstitial and substitutional solute effects in intermetallics, TMS , Warrendale Warrendale 1998, pp. 227-246.

[23] H. Clemens, Mayer, S., Design, Processing, Microstructure, Properties, and Applications of Advanced Intermetallic TiAl Alloys, Adv Eng Mater, 15 (2013) 191-215.

[24] C. Scheu, Stergar, E., Schober, M., Cha, L., Clemens, H., Bartels, A., Schimansky, F. P., Cerezo, A., High carbon solubility in a γ-TiAl-based Ti–45Al–5Nb–0.5C alloy and its effect on hardening, Acta Mater, 57 (2009) 1504-1511.

[25] R. Gerling, H. Clemens, F.P. Schimansky, Powder metallurgical processing of intermetallic gamma titanium aluminides, Adv. Eng. Mater. 6 (2004) 23-38.

[26] H. Gabrisch, A. Stark, F.P. Schimansky, L. Wang, N. Schell, U. Lorenz, F. Pyczak, Investigation of carbides in Ti–45Al–5Nb–xC alloys ($0 \leq x \leq 1$) by transmission electron microscopy and high energy-XRD, Intermetallics, 33 (2013) 44-53.

[27] L. Wang, H. Gabrisch, U. Lorenz, F.-P. Schimansky, A. Stark, F. Pyczak, Perovskite Ti3AlC Carbide Splitting in High Nb Containing TiAl Alloys, MRS Proceedings, 1760 (2014).

[28] A. Menand, A. Huguet, A. Nérac-Partaix, Interstitial solubility in γ and α2 phases of TiAl-based alloys, Acta Mater, 44 (1996) 4729-4737.

[29] T. Klein, M. Schachermayer, F. Mendez-Martin, T. Schöberl, B. Rashkova, H. Clemens, S. Mayer, Carbon distribution in multi-phase γ-TiAl based alloys and its influence on mechanical properties and phase formation, Acta Mater, 94 (2015) 205-213.

[30] J.C. Schuster, H. Nowotny, C. Vaccaro, The ternary systems: CrAlC, VAlC, and TiAlC and the behavior of H-phases (M_2AlC), J Solid State Chem, 32 (1980) 213-219.

[31] M.A. Pietzka, J.C. Schuster, Summary of constitutional data on the Aluminum-Carbon-Titanium system, J Phase Equilib, 15 (1994) 392-400.

[32] V.T. Witusiewicz, B. Hallstedt, A.A. Bondar, U. Hecht, S.V. Sleptsov, T.Y. Velikanova, Thermodynamic description of the Al–C–Ti system, Journal of Alloys and Compounds, 623 (2015) 480-496.

[33] L. Cornish, G. Cacciamani, D. Cupid, J. De Keyzer, Aluminium – Carbon – Titanium, in: G. Effenberg, S. Ilyenko (Eds.) Refractory metal systems, Springer Berlin Heidelberg, 2009, pp. 63-101.

[34] Al-C-Ti Isothermal Section of Ternary Phase Diagram, in: Pierre Villars, Material Phases Data System (MPDS), CH-6354, Springer-Verlag GmbH, Heidelberg, 2014.

[35] R. Ayer, R. Ray, J.C. Scanlon, Analytical microscopy of a γ-TiAl composite containing a carbide phase, Scr Metall Mater, 26 (1992) 1337-1342.

Tables

Table 1 Oxygen and nitrogen contents in TiAl specimens after HIPing and casting.

Alloy (at.%)	O (μg/g)	N (μg/g)
Ti-45Al-5Nb-0.5C	381	56
Ti-45Al-5Nb-0.75C	512	48
Ti-45Al-5Nb-1.0C	586	39
Ti-45Al-0.5C	543	134
Ti-51Al-5Nb	311	79
Ti-51Al-5Nb-0.01C	307	122
Ti-51Al	234	25
Ti-51Al-0.01C	357	51

Table 2 Nominal alloy compositions, primary phase contents and heat treatment conditions of the investigated TiAl alloys

Alloy (at.%)	Primary phase contents (wt.%)	Heat treatment conditions
PM Ti-45Al-5Nb-0.5C	82.9 γ + 17.1 α_2 + rare P [26]	@ 800, 900, 1000 °C for 24, 48, 96, 168 h, FC [15]
		@ 1250 °C for 5 h, OQ + @ 800 °C for 24, 48, 96, 168, 1104, 5000 h, FC
PM Ti-45Al-5Nb-0.75C	82.5 γ + 17.5 α_2 + a few P + few H	@ 800 °C for 24, 48, 96, 168 h, FC; @ 900, 1000 °C for 24, 48, 96, 168 h, FC [15]
		@ 1250 °C for 5 h, OQ + @ 800 °C for 24, 48, 96, 168, 1054 [15], 5000 h, FC
PM Ti-45Al-5Nb-1.0C	83.5 γ + 16.5 α_2 + a few P + a few H	@ 800 °C for 24, 48, 96, 168, 4800 h, FC; @ 900, 1000°C for 168 h, FC
PM Ti-45Al-0.5C	75.1 γ + 24.9 α_2	@ 1250 °C, 5h, OQ + @ 800 °C for 24, 48, 96, 168, 1054, 5000 h, FC
Cast Ti-51Al-5Nb-xC (x=0, 0.01, 0.05, 0.5)	γ + trace amount (≈1-2) α_2 + a few P	@ 800 °C for 24, 48, 96, 168, 5000 h, FC
Cast Ti-51Al-xC (x=0, 0.01, 0.025)	γ + trace amount (≈1-2) α_2	@ 800 °C for 168 h, FC

FC means furnace cooling, OQ means oil quenching.

Table 3 α_2 phase fraction in TiAl alloys measured by HEXRD

Heat treatment conditions	α_2 phase fraction (wt.%)			
	Ti-45Al-5Nb-0.5C [15]	Ti-45Al-5Nb-0.75C [15]	Ti-45Al-5Nb-1.0C	Ti-45Al-0.5C
@ 800 °C	15.1 (24 h) →13.6 (168 h)	14.9 (24 h) →13.3 (168 h)	13.4 (24 h) →11.7(168 h) →11.2 (1054 h)	/
@ 900 °C,	15.3 (24 h) →13.8 (168 h)	12.8 (24 h) →12 (168 h)	10.7 (168 h)	/
@ 1000 °C,	13.7 (24 h) →13.8 (96 h)	11.6 (24 h) →10.8 (168 h)	9.7 (168 h)	/
@ 1250 °C, 5 h + @ 800 °C	16.5 (24 h) →15.4 (168 h) →14.6 (1104 h)	16.4 (24 h) →14.1 (168 h) →12.6 (1054 h)	/	20.8 (1054 h)
@ 1250 °C, 5 h + @ 900 °C	15 (24 h) →14.4 (168 h)	13.1 (24 h) →12 (168 h)	/	/
@ 1250 °C, 5 h + @ 1000 °C	14.2 (24 h) →12.7 (168 h)	11.7 (24 h) →10.1 (168 h)	/	/

"/" means that the experiments were not carried out

Table 4 Summarization of the carbide existence in TiAl alloys at different annealing conditions

Alloy, at.%	@ 800 °C	@ 900 °C	@ 1000 °C
PM Ti-45Al-5Nb-0.5C	P (24-5000 h)	P (24-168 h)	P dissolve
PM Ti-45Al-0.5C	P (24-5000 h)	/	/
PM Ti-45Al-5Nb-0.75C	P (24-5000 h)	P (24-168 h)	P (24-168 h)
PM Ti-45Al-5Nb-1.0C	P + H (24-5000 h)	P + H (24-168 h)	P + H (24-168 h)
Cast Ti-51Al-5Nb-0.01C	P (168 h)	/	/
Cast Ti-51Al-5Nb-0.05C	P+ H (168 h)	/	/
Cast Ti-51Al-5Nb-0.5C	P + H (24-168 h) H (5000 h)	/	/
Cast Ti-51Al-0.01C	P + H (168 h)	/	/
Cast Ti-51Al-0.025C	P (168 h)	/	/

"/" means that the experiments were not carried out

Figure captions

Fig. 1 SEM micrographs (back-scattered electron mode) of the Ti-45Al-5Nb-0.5C alloy after (a) annealing treatment at 800 °C for 168 h, and (b) solution treatment at 1250 °C for 5 h and annealing treatment at 800 °C for 168 h.

Fig. 2 TEM micrographs of P-type carbides in the γ matrix of the TiAl alloys after solution treatment at 1250 °C for 5 h and annealing treatment at 800 °C for different times. All images have the same magnification.

Ti-45Al-0.5C: (a) 168 h ($[001]_\gamma$), (c) 1054 h ($[001]_\gamma$) and (e) 5000 h ($[100]_\gamma$);

Ti-45Al-5Nb-0.5C: (b) 168 h ($[001]_\gamma$), (d) 1054 h ($[001]_\gamma$) and (f) 5000 h ($[100]_\gamma$).

Fig. 3 TEM micrographs of carbides in the Ti-45Al-5Nb-1.0C alloy after annealing at 800 °C.

P-type carbides after annealing for (a) 24 h, (b) 48 h, (c) 96 h, (d) 1054 h, (e) 5000 h, together with the diffraction pattern. H-type carbide after annealing for (f) 24 h, together with its diffraction pattern.

Fig. 4 TEM micrographs of the carbides in the γ matrix of the Ti-51Al-5Nb-0.5C alloy.

P-type carbides: (a) with a needle-like shape after ageing at 800 °C for 24 h, (b) start to split after ageing at 800 °C for 48 h, (c) split after ageing at 800 °C for 168 h and conglomerates with smaller carbide sub-particles are visible;

H-type carbides with a plate-like shape form in the γ matrix together with the diffraction pattern after ageing at 800 °C for (d) 96 h and (e) 5000 h.

Fig. 5 TEM micrographs of H-type carbides together with diffraction patterns at grain boundaries in the Ti-51Al-5Nb-0.5C alloy. (a) at γ/γ grain boundaries after annealing at 800 °C for 24 h, (b) and (c) at γ/γ grain boundaries after annealing at 800 °C for 168 h. All images have the same magnification.

Fig. 6 TEM micrographs of (a) P-type and (b) H-type carbides together with diffraction patterns in the Ti-51Al-0.01C alloy after annealing at 800 °C for 168 h.

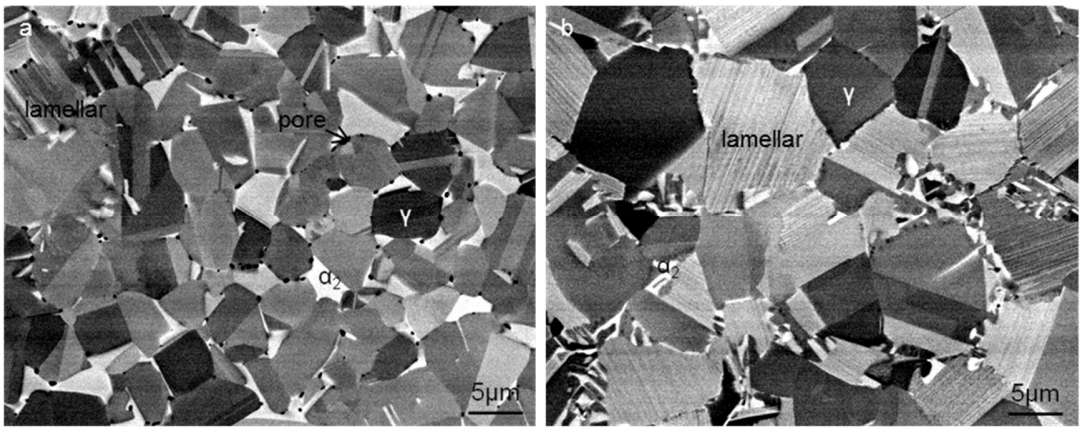

Figure 1

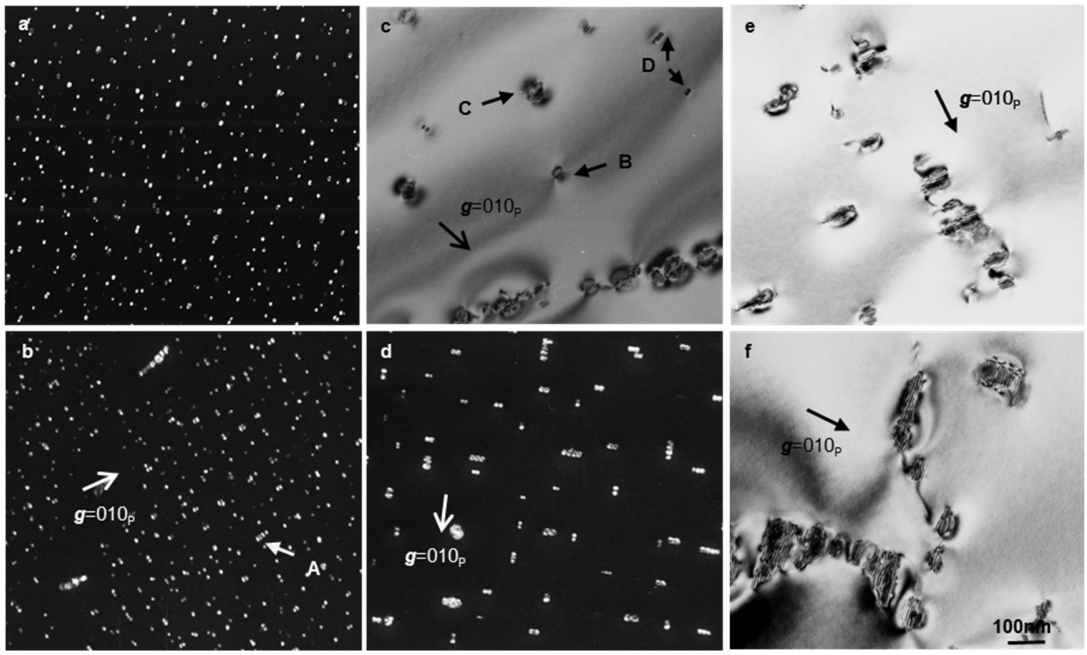

Figure 2

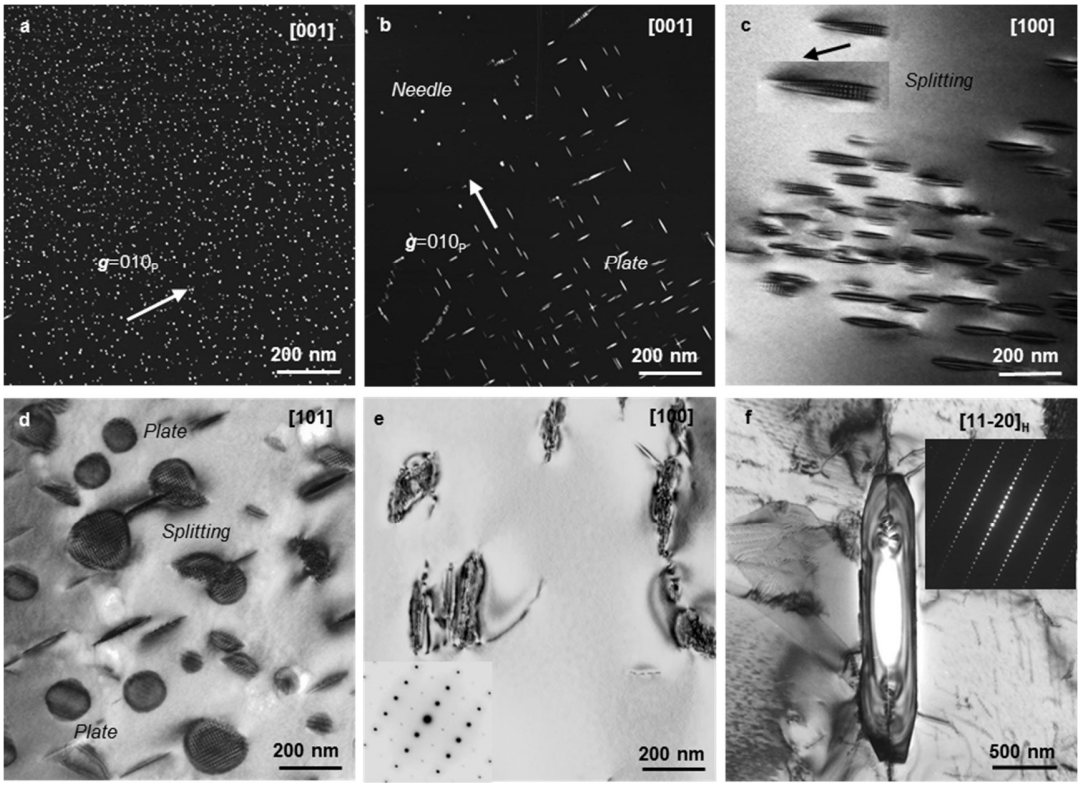
a
[001]
g=010P
200 nm
b
[001]
Needle
g=010P
Plate
200 nm
c
[100]
Splitting
200 nm
d
Plate
[101]
Splitting
Plate
200 nm
e
[100]
200 nm
f
[11-20]H
500 nm

Figure 3

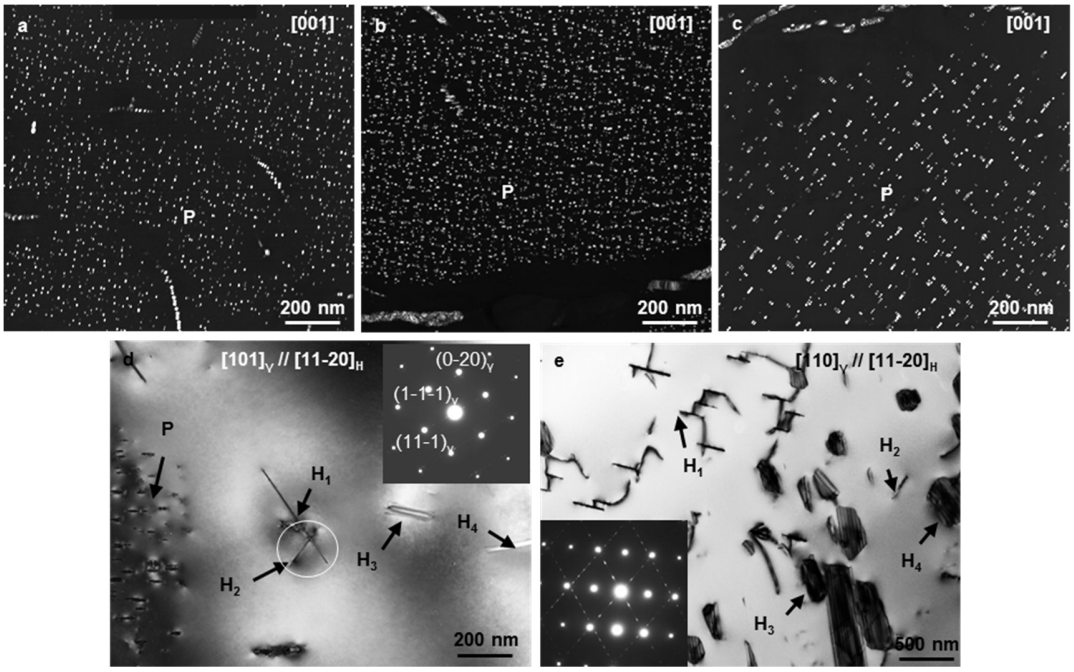
a
[001]
P
200 nm
b
[001]
P
200 nm
c
[001]
P
200 nm
d
[101]V // [11-20]H
(0-20)V
(1-1-1)V
(11-1)V
P
H1
H2
H3
H4
200 nm
e
[110]V // [11-20]H
H1
H2
H3
H4
500 nm

Figure 4

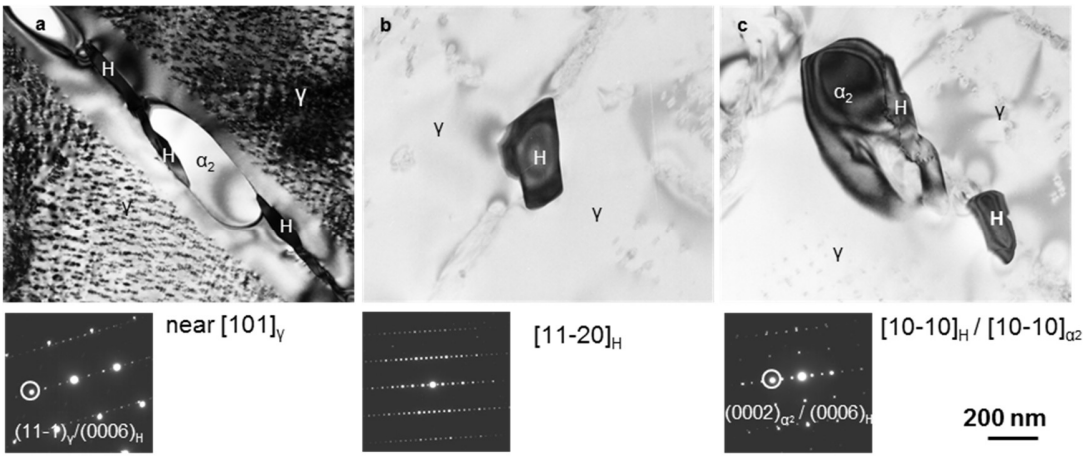
a
H
γ
H
α2
γ
H
b
γ
H
γ
c
α2
H
γ
H
γ
near [101]γ
[11-20]H
[10-10]H / [10-10]α2
(11-1)γ/(0006)H
(0002)α2 / (0006)H
200 nm

Figure 5

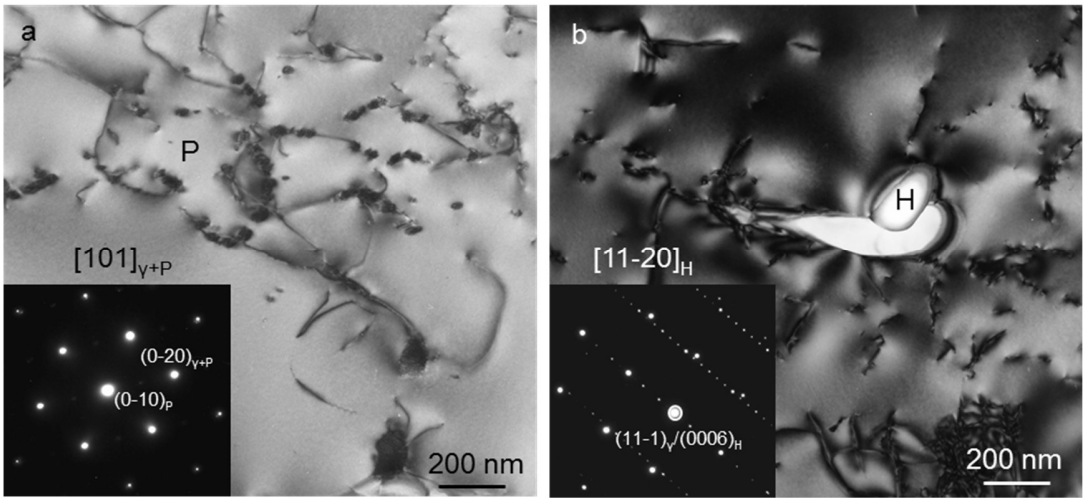

Figure 6